

An Adsorption Study of Removal of Heavy Metals Using Environment Friendly Agro Based Materials

Jaisankar viswanathan (✉ vjaisankar@gmail.com)

Presidency College <https://orcid.org/0000-0003-0894-4703>

K Aswini

Presidency College

K Deepa

College for women

N Suganya

College for women

V Jaisankar

Presidency College

Research Article

Keywords: Graphene oxide, Polymer composite, adsorption, heavy metals, kinetic Models

Posted Date: June 1st, 2021

DOI: <https://doi.org/10.21203/rs.3.rs-550253/v1>

License:   This work is licensed under a Creative Commons Attribution 4.0 International License.

[Read Full License](#)

An adsorption study of removal of heavy metals using environment friendly agro based materials

Aswini K¹, Deepa K², Suganya N² and Jaisankar V^{1*}

¹Department of chemistry, Presidency College (Autonomous),
Chennai-600 005, Tamil Nadu, India

²Department of chemistry, Ethiraj College for women (Autonomous),
Chennai-600 005, Tamil Nadu, India

*Corresponding author: vjaisankar@gmail.com

Abstract

The tremendous increase in the usage of heavy metals over the past few decades resulted in an increased flux of metallic substances in the aquatic environment which requires special concern because of their persistency. The investigation illustrates the removal of heavy metals from waste water by coconut husk based polymer/graph The method of graphene oxide (GO) synthesis involves the single-step reforming of Coconut husk agricultural waste material by oxidation under muffled atmosphere condition. ene oxide composites (CHGO) which is expected to act as good adsorbent materials. The graphene oxide (CHGO) and the corresponding composites PVP/CHGO and PEG/CHGO were characterized by Fourier transform infrared (FTIR), X-ray Diffraction Analysis (XRD) and scanning electron microscope (SEM) analysis. The adsorption study of Coconut husk Graphene oxide (CHGO) and its composites *viz.*, Polyvinylpyrrolidone (PVP)/ Coconut husk Graphene oxide nanocomposite (PVP/CHGO) and Polyethyleneglycol (PEG)/ Coconut husk Graphene oxide nanocomposite (PEG/CHGO) was carried out for the removal of heavy metals from simulated waste water and results were compared. The performance analysis was carried out as a function of various operating parameters, such as initial concentration of metal ion, adsorbent dosage, contact time, and pH. The studies revealed that materials are effective in removal of heavy metals. The Pseudo-first, Pseudo-second order and Elovich kinetic Models were used to analyse the adsorption equilibrium.

Keywords: Graphene oxide, Polymer composite, adsorption, heavy metals, kinetic Models.

1.INTRODUCTION rece

In environment research, the removal of heavy metals by adsorption using agro based materials emerged as a powerful technology to treat wastewater due to its easy operating requirements and low cost. In this context, Graphene oxide (GO) has attracted major research attention due to the wide range of envisaged applications across several scientific and engineering fields including physics, chemistry, biology, and medicine [1-5]. The original method for the preparation of GO is based on the addition of potassium chlorate to a slurry of graphite in fuming nitric acid [6]. This synthetic protocol can be improved by using concentrated sulfuric acid as well as fuming nitric acid and adding the chlorate in multiple aliquots over the course of the reaction [7]. In the commonly used Hummers' method [8], graphite is oxidized throughout treatment of KMnO_4 and NaNO_3 in concentrated H_2SO_4 acid all these procedures involve the generation of NO_2 , N_2O_4 , and ClO_2 , toxic gases which are also explosive. Also, various techniques such as mechanical exfoliation techniques, and Chemical Vapor Deposition (CVD) techniques and other chemical techniques have been developed for the synthesis of graphene and graphene oxide materials. Many of these techniques are highly sophisticated and expensive [9]. Most of the commercially available GO samples were prepared by Hummers' method or a modified version of it. In compare with the Hummers' method, our method is more environment friendly as it avoids toxic gas emission during synthesis. The synthesis technique reported here is a quite efficient asset for demonstrating a new procedure for the production of graphene oxide from agro waste in simple steps. This simple and low-cost process could lead to new opportunities for cost-effective production of GO [10,11]. Here, we reported on the synthesis of graphene oxide by directly oxidizing coconut husk under muffled atmosphere. The GO produced by this method is called COMA-GO (coconut husk oxidized under muffled atmosphere for graphene oxide). Furthermore, the structural characteristics of the obtained product are confirmed by X-ray diffraction, Fourier transmission infrared spectroscopy, and High Resolution Scanning Electron Microscopic Analysis (HRSEM) and Raman spectroscopy. There is very little effort has been done to use PVP and PEG alone as an adsorbent without forming any nanocomposite for the removal of heavy metals from aqueous solution. Hence, our present effort has been made to evaluate polymer composites as an effective adsorbent for the removal of heavy metals from aqueous solution.

2. Materials

The materials used for the preparation of simulated wastewater were Copper Nitrate, Lead Nitrate and Cadmium Nitrate purchased from Merck, was of purity 98-99%. The H_3PO_4 , HCl and NaOH. All other chemicals used were analytical grade and used as such. The coconut husk is collected from agriculture waste.

3. Experimental

3.1 Preparation of Graphene oxide from Coconut husk

Coconut husk is a type of agricultural waste. It was washed repeatedly in tap water and distilled water thoroughly to remove dust and other impurities and then oven dried at $100\pm 5^\circ C$ for 24 hours. The Coconut husk was crushed and ground well in order to produce powder. This crushing and separating process was repeated several times to obtain fine powder. About 0.5 g of ground Coconut husk powder mixed with 0.1 g of ferrocene, placed in a crucible and kept in muffle furnace at $300^\circ C$ for 10 min under atmospheric conditions. The as-produced black solid (CHGO) Coconut husk based graphene oxide was collected at room temperature [12].

3.2 Preparation of polymer nanocomposites (PVP/RHGO and PEG/CHGO)

The powdered CHGO was treated with an emulsion of readily available synthetic polymer-PVP. Nine parts by weight of graphene oxide (CHGO) was mixed with one part by weight of PVP to form a semisolid mass. The agglomerated product was dried and ground into fine powder. The adsorbent was dried at $110^\circ C$ for 2 hours. This powder was then used as an adsorbent material. As mentioned above the other polymer composites are prepared using PEG and named as PEG/CHGO.[13-15].

3.3. Preparation of Simulated wastewater

The 1000 ppm standard solutions of Copper, Cadmium and lead were prepared by dissolving measured quantities of their respective salts in distilled water. The simulated wastewater was prepared by using measured amount of standard solutions. The concentration of Cu, Cd and Pb were 20 ppm, 10 ppm and 5 ppm respectively.

3.4. Adsorption experiment

Adsorption experiment was carried out by measuring 25mL of the simulated wastewater sample and poured into a 100 mL conical flask. 0.6 g of the synthesized CHGO,

PVP/CHGO and PEG/CHGO nanocomposite were added to different conical flask containing 25mL of wastewater. The conical flask containing the adsorbent and the wastewater was placed on a rotary shaker and shook at 120 rpm at a room temperature of (30°C) for a period of 150 min to ensure equilibrium. The suspension was filtered using Whatman No.1 filter paper. The concentration of remaining metal ions in the adsorption medium was determined by UV-Visible spectrophotometer [16-18].

The metal concentration (mg/g) of the adsorbent phase (q_e) and the removal efficiency (%) of the adsorbent preparations was calculated using the following equations respectively:

$$q_e = \frac{C_0 - C_e}{C_0} \times V \quad \text{----- (1)}$$

$$\text{Removal efficiency (\%)} = \frac{C_0 - C_e}{C_0} \times 100 \text{----- (2)}$$

Where C_0 and C_e are the concentrations (mg/l) of metals ions before and after adsorption respectively, V (ml) is the volume of the metal ions and m (g) is the mass of the adsorbent.

3.4.1. Effect of Contact Time: To study the effect of contact time 0.2 gram of adsorbent is taken in 25ml of aqueous solution of initial metal ion concentration 20, 10, 5 mg/ L, at the shaking was provided for 30 minutes. The experiment was repeated for different time intervals like 30, 60, 90, 120, 150 minutes at constant agitation speed 120 rpm, after each interval of time, the sample was filtered and was analyzed for determination of optimum contact time.

3.4.2. Effect of Adsorbent Dose: The effect of adsorbent dosage on the amount of Metal ion adsorbed was obtained by agitating 25ml of metal ion solution of 20, 10, 5mg/ L, separately with 0.2, 0.4, 0.6, 0.8 and 1.0 grams of adsorbent at room temperature for optimum shaking time at constant agitation speed. The filtered solution of Metal was analyzed with the help of by UV-Visible spectrophotometer.

3.4.3. Effect of pH: The effect of pH was studied using the stock solution of concentration 20, 10, 5mg/ L, was treated with dilute acid in order to maintain the pH value to 2, 4, 6 and base to maintain the pH up to 10. The acid used was freshly prepared HCl and base was NaOH. After setting the pH of the ranges 2, 4, 6, 8 and 10 in different flasks, 25ml stock solution and 0.2 g CHGO, PVP/CHGO and PEG/CHGO was added into each Conical flask

and allowed to undergo shaking for 150 min. The filtered solution of Metal ion was analyzed with the help of by UV-Visible spectrophotometer.

4. CHARACTERISATION METHODS

The preparation of Graphene oxide from Coconut husk CHGO, PVP-CHGO and PEG/CHGO composites were characterized by spectral methods. A principle of FT-IR spectrophotometry is it relies on the fact that the most molecules absorb light in the infra-red region of the electromagnetic spectrum. X-ray diffraction patterns were collected from 10° to 60° in 2θ by a XRD with CuKα (λ = 0.1542 nm) radiation on a D8 Advance (Bruker-AXS) diffract meter. Surface morphology of samples was analyzed by scanning electron microscope (HR-SEM, S2600 HITACHI). Raman analysis was carried out at room temperature using a Raman spectroscopy (Renishaw InVia, UK) with a 514 nm laser light [19-23]. UV/Visible Scanning Spectrophotometer SHIMADZU 1800 using pure components or mixture of components can be used as standard samples [16,17,24].

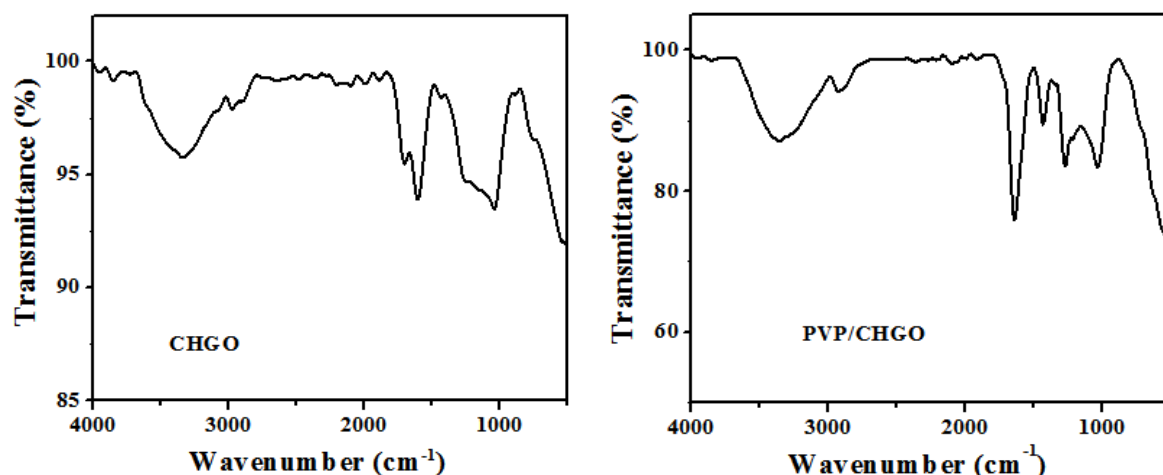
The Scherrer's equation[25]

$$D = \frac{0.89\lambda}{\beta \cos \theta} \quad \text{-----} \quad (3)$$

Where λ is the wavelength (CuKα), β the full width at half-maximum (FWHM) of the CHGO, PVP/CHGO and PEG/CHGO nanocomposite.

5. RESULT AND DISSCUSSION

5.1 Fourier Transform Infrared (FTIR) Spectroscopy



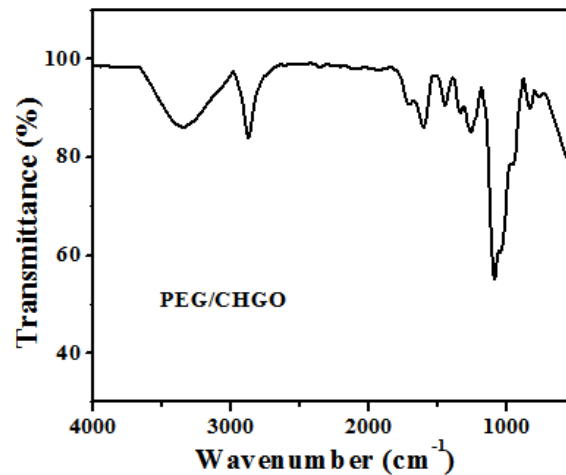


Fig.1. FT-IR spectra recorded for CHGO, PVP/CHGO and PEG/CHGO

The FTIR spectra of graphene oxide prepared from rice husk, sugarcane bagasse and coconut husk presented in Fig.1. The broad band located at about $3200 - 3500 \text{ cm}^{-1}$ is assigned to the O–H stretching vibrations of water absorbed on RHGO, SBGO and CHGO. The band at 1598 cm^{-1} may be attributed to asymmetric C=O stretching of unoxidised graphitic domains. The band at 1060 cm^{-1} can be attributed to C–O (epoxy) groups. The band at 2960 cm^{-1} attributed to C–H stretching of aliphatic group. The band at 878 cm^{-1} corresponds to the contribution from C–H bond vibration in aromatic compounds. The band at 1425 cm^{-1} the stretching vibration of the CN groups of PVP. The stretching vibration of C–H all 948 and 2879 cm^{-1} corresponding to $-\text{CH}_2$ of PEG. The bands of CH-CH₂ asymmetric and symmetric stretching found at 2908 cm^{-1} and 2873 cm^{-1} respectively. The C–C and C–O stretching vibration is observed at 1133 cm^{-1} and 1287 cm^{-1} respectively.

5.2. X-ray Diffraction Analysis (XRD):

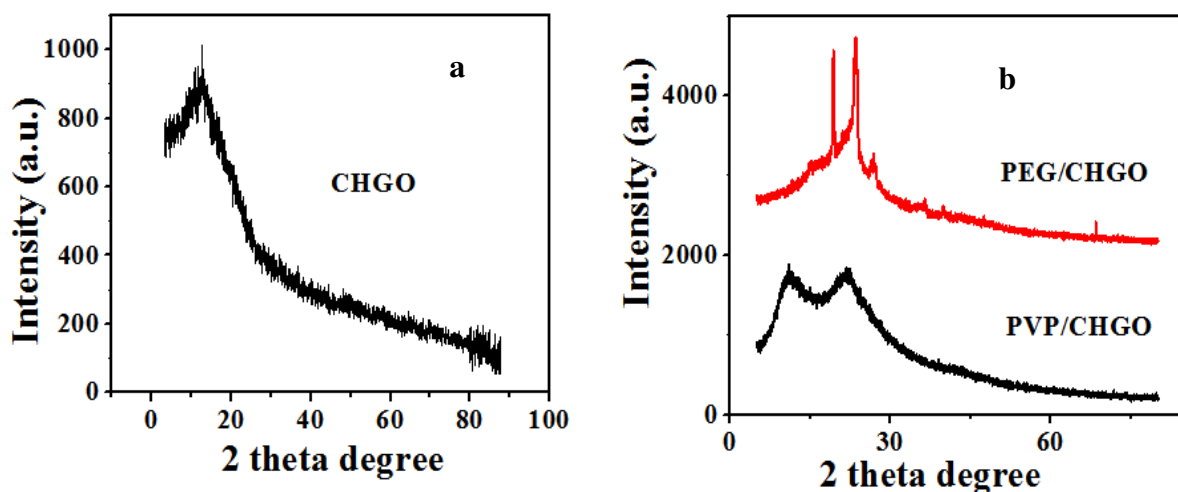


Fig.2. X-ray diffraction pattern of Coconut husk (a), CHGO, (b) PVP/CHGO and (c), PEG/CHGO

The XRD pattern of graphene oxide prepared from agricultural waste materials such as coconut husk was displayed in Figure.2(a). The structural and chemical analysis of coconut husks is clearly described by previous investigators. In this study, we have presented the XRD pattern of the CHGO which is shown in Figure 2(a). The peak at $2\theta = 12.79^\circ$ indicates that the agricultural coconut husk is fully oxidized into graphene oxide with the interlayer distance of 0.78 nm. The agricultural coconut husk is fully oxidized into graphene oxide. The 2θ peaks of the CHGO obtained by the single-step oxidation of coconut husk are consistent with the results of previous studies [26,27]. This XRD pattern can be attributed to well graphitized two-dimensional structures made of GO nano sheets.

5.3. High Resolution Scanning Electron Microscopic Analysis (HRSEM)

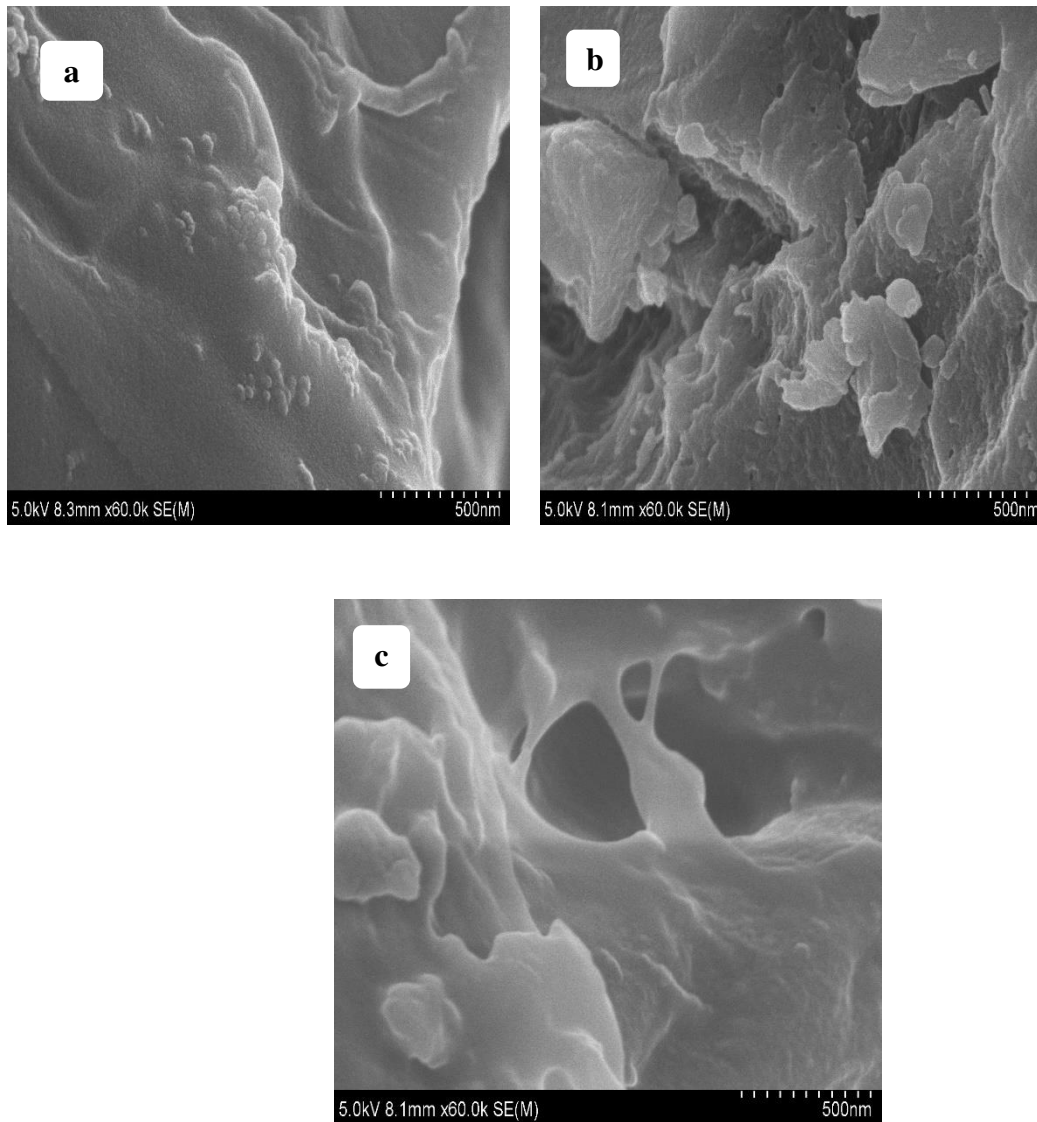


Fig.3. HRSEM images of (a) CHGO, (b) PVP/CHGO and (c) PEG/CHGO

The HRSEM image (Fig. 3 (a)) shows that few layered graphene oxides are formed, although the HRSEM image suggesting the multi-layer nature of the presently prepared graphene nanosheets. The scanning electron micrograph for the PVP/CHGO and PEG/CHGO nanocomposites materials (Fig.3 (b) and (c)) demonstrates that a homogeneous system with a micrometer order of magnitude was obtained. The functionalization, GO exhibits a three-dimensional network of randomly oriented sheet-like structures with a wrinkled texture and hierarchical pores with a wide size distribution.

5.4. Fourier Transform Raman (FT-Raman)spectroscopy

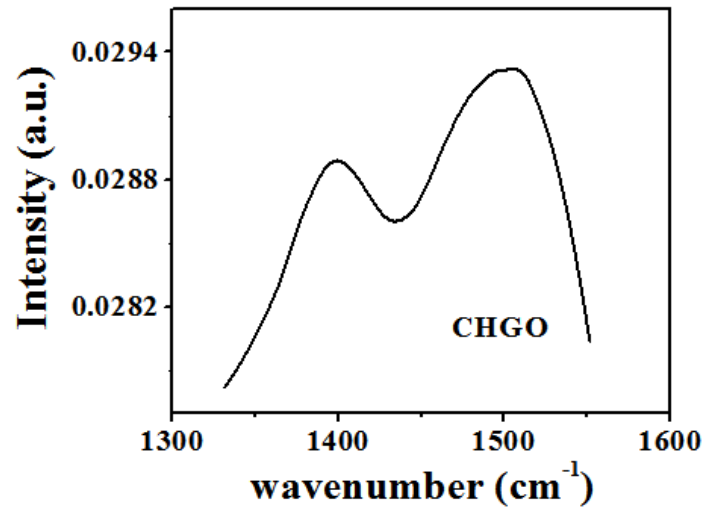


Fig.4. Raman spectrum of GO form Coconut husk (CHGO)

The Raman spectrum of graphene oxide synthesized from coconut husk [27] is shown in Figure 4. GO displayed two prominent peaks at 1377 and 1590 cm^{-1} , which were corresponded to the D and G bands, respectively. The two D and G bands at 1377 cm^{-1} and 1590 cm^{-1} [28] indicate the clear sp^2 carbon hybridization in the observed multi-layer stacks [29]. Thus, ID/IG peak intensity ratios are assigned to lower defects/disorders. Raman spectra show an intensity ratio of ID/IG at 0.9853 for GO which is in line with previous investigations [27, 30, 31].

5.5. Adsorbent method

5.5.1. Effect of Contact Time

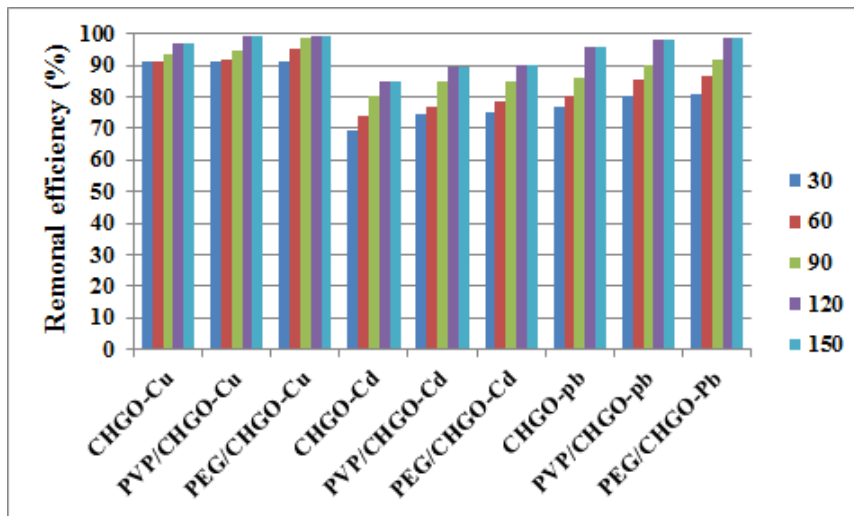


Fig.5. Effect of Contact time on adsorption of Lead, Copper and Cadmium metal ions pH=6 (dose= 0.6)

The CHGO, PVP/CHGO and PEG/CHGO nanocomposites as an adsorbent dosage of 0.6 g. The is shown in fig 5. The percentage removal of metal ions approached equilibrium within 120 min of adsorption capacity of Copper 96.66, 99.34, and 99.51, and 84.92, 89.31, and 89.95 for Cadmium, 95.99, 98.19, and 98.39 of lead; removal of metal ions respectively. This may be due to the heterogeneity obtained by the presence of functional groups on the surface of the polymer composites. This may be due to the orderly arrangement of polymer matrix [32, 33].

5.5.2. Effect of Adsorbent Dosage

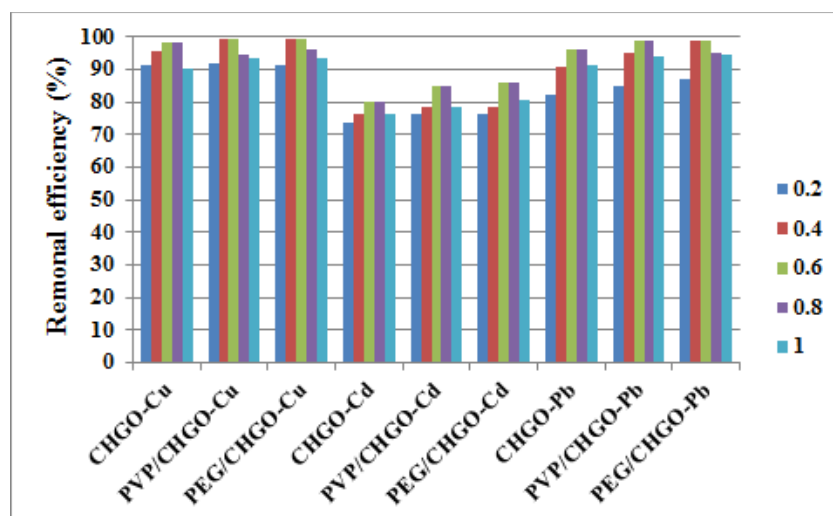


Fig.6. Effect of Adsorbent dosage on adsorption of Lead, Copper and Cadmium metal ions pH=6 (Contact time= 120)

The effect of dosage of adsorbent CHGO, PVP/CHGO and PEG/CHGO composites at a Contact time of 120 min is shown in fig 6 .The percentage removal of metal ions approached equilibrium within 0.6 g of adsorption capacity 96.24 and 98.67 of lead; Copper 97.98; 80.27, 84.79, and 85.87 for cadmium and the 0.4g adsorption capacity PEG/CHGO 98.71 of lead and PVP/CHGO, PEG/CHGO Copper 99.26 and 99.48 removal of metal ions respectively, after which further increase in adsorbent dosage[34,35], brought no increase in adsorption, which was as a result of overlapping of adsorption sites due to overcrowding of adsorbent particles[36].

5.5.3. Effect of pH

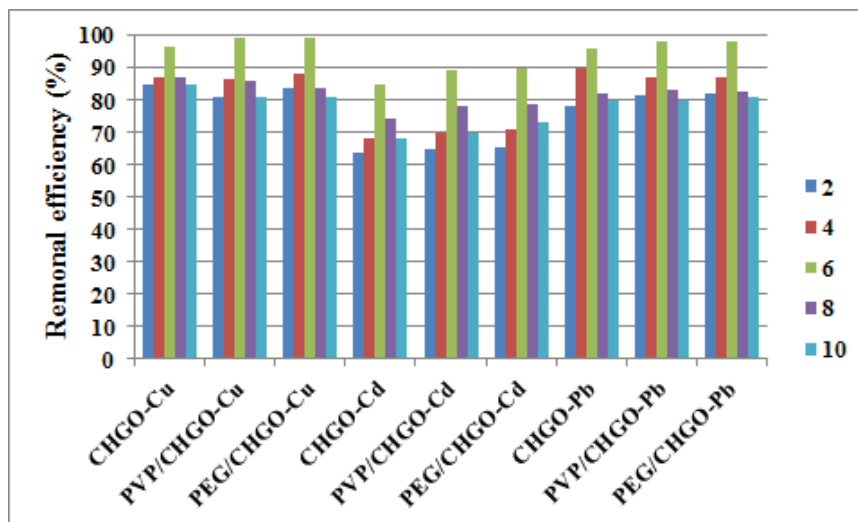


Fig.7. Effect of pH on adsorption of Lead, Copper and Cadmium metal ions pH=6 (dose= 0.6)

The CHGO, PVP/CHGO and PEG/CHGO composites at a Contact time of 120 min with adsorbent dosage of 0.6gm at pH 6, shows maximum removal of Copper 97.67, 99.58 and 99.51; 84.93, 89.26 and 89.97 for Cadmium 95.98, 98.10, and 98.39 for lead respectively. From the results above, it reveals that the adsorption capacity of CHGO, PVP/CHGO and PEG/SBAC depends on the pH of Stimulated waste water. At lower pH values, the large number of H⁺ ions neutralizes the negatively charged adsorbent surfaces, thereby reducing the hindrance of the metal ions. At high pH values, the reduction in adsorption may be due to the abundance OH⁻ ions causes increased hindrance to the diffusion of metal ions [37]. From fig 7. the percentage removal of metal ions increases sharply and

attain maximum at pH 6, for CHGO, PVP/CHGO and PEG/CHGO composites. Thereafter, the percent removal decreases with increase in pH. There is no significant adsorption takes place beyond pH=6.

5.6. ADSORPTION KINETICS:

In order to investigate the mechanism of total copper, cadmium and lead adsorption onto adsorbents three kinetic models were studied; Lagergren's first –order, Pseudo – second order and Elovich kinetic models [38].

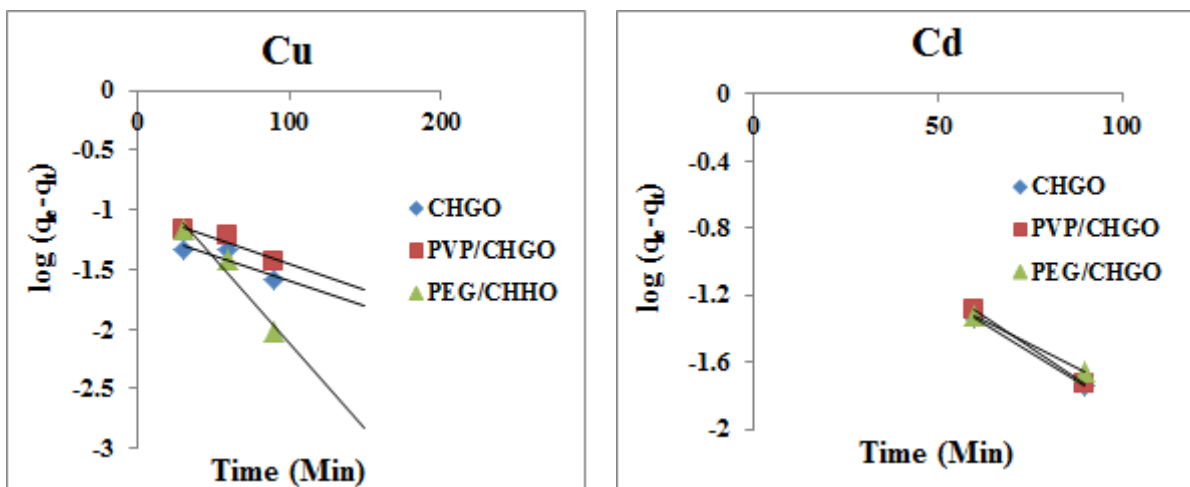
5.6.1. LAGERGREN'S FIRST-ORDER KINETIC MODEL

The pseudo-first-order kinetic model of lagergren is more suitable for lower concentration of solute and its linear form is [39]

$$\log(q_e - q_t) = \log q_e - \frac{k_1}{2.303} t \quad \text{----- (6)}$$

Where, q_t (mg g^{-1}) is the amount of adsorbate adsorbed at time t [min]; q_e [mg g^{-1}] is the adsorption capacity in the equilibrium; k_1 [min^{-1}] is the rate constant of pseudo-first-order model.

The value of k_1 and q_e for CHGO, PVP/CHGO and PEG/CHGO nanocomposite adsorbents was determined from the plot of $\log [q_e - q_t]$ vs. time which is shown in Fig.8. The correlation coefficient, R^2 [40, 41] for CHGO, PVP/CHGO and PEG/CHGO nanocomposite was presented in Table.1, 2 and 3.



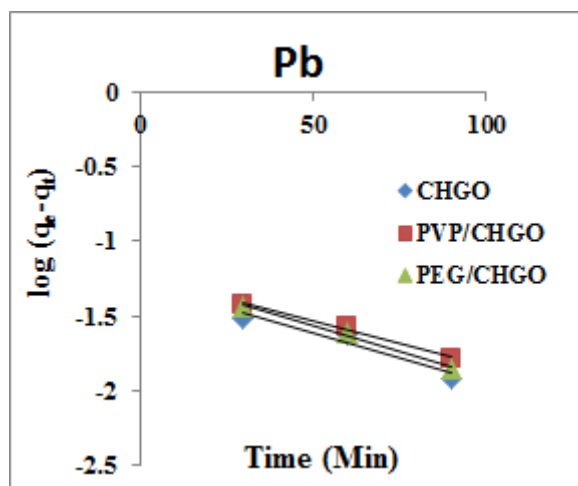


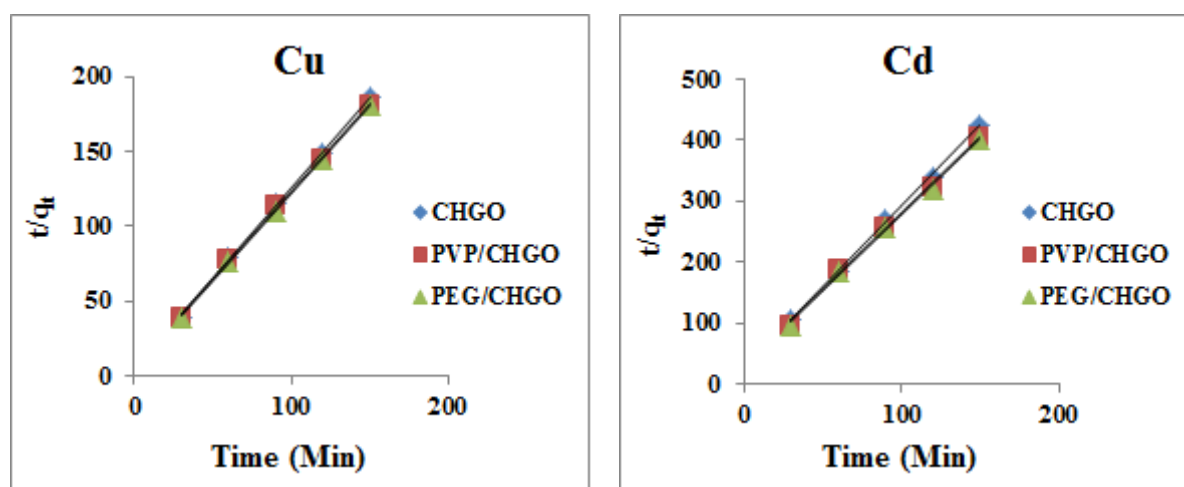
Fig.8.Lagergren first-order –kinetic model for the adsorption of removal Cu, Cd and Pb metal ions with CHGO, PVP/CHGO and PEG/CHGO nanocomposite

5.6.2. PSEUDO-SECOND-ORDER KINETIC MODEL

Adsorption kinetic was explained by the pseudo-second-order model expressed as following linear equation [42, 43]

$$\frac{t}{q_t} = \frac{1}{k_2 q_e^2} + \frac{t}{q_e} \quad \text{----- (4)}$$

Where, k_2 is the second order rate constant [$\text{g mg}^{-1} \text{min}^{-1}$]. The values of k_2 for removal of Cu, Cd and Pb by CHGO, PVP/CHGO and PEG/CHGO adsorbents was calculated from the slopes of the respective linear plots of t/q_t vs. t [Fig.9.]. The correlation coefficients, R^2 values for CHGO, PVP/CHGO and PEG/CHGO respectively suggest a strong relationship between the parameters and also explain that the process follows pseudo second order kinetics [Table.1,2 and 3].



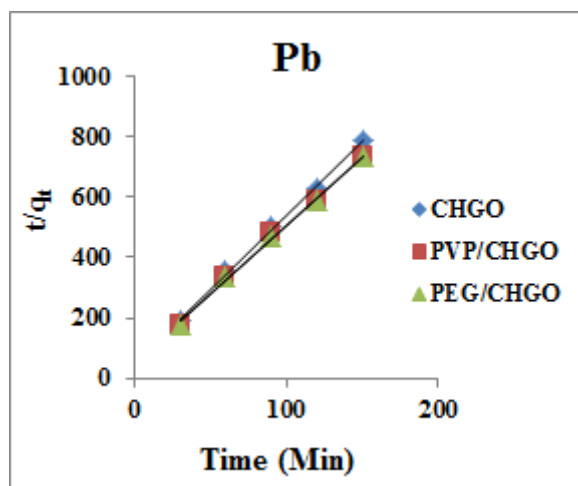


Fig.9. Pseudo second-order –kinetic model for the adsorption of removal Cu, Cd and Pb metal ions with CHGO, PVP/CHGO and PEG/CHGO nanocomposite

5.6.3. ELOVICH KINETIC MODEL

Elovich model suggests that the chemisorptions, i.e. a chemical reaction, are probably the mechanism that controls the rate of adsorption. This model can be applied with success in liquid solution and the linear form of the Elovich equation is [44]:

$$q_t = \frac{1}{\beta} \ln \alpha \beta + \frac{1}{\beta} \ln t \text{----- (5)}$$

Where, α [mg g^{-1}] is the initial sorption rate and β [g mg^{-1}] is the desorption constant. The values of α and β can be calculated from the slope and intercept of the plot of q_t versus $\ln t$ show in Fig.10.

As can be seen from the fig.9, the values of R^2 are closer to unity for pseudo second order model than pseudo first order model and Elovich model is shown in table.1, 2 and 3. Thus, adsorption of total metals onto adsorbent follows the pseudo second order model. Furthermore, values of q_e (cal) calculated from pseudo second order model were in good agreement with experimental values, q_e (exp) than those calculated from pseudo first order. The values of R^2 for pseudo first order and Elovich model are lower than the pseudo second order model and thus indicate that pseudo first order and Elovich model cannot be adequate to describe the kinetic of adsorption of Cu, Cd and Pb metal ions onto CHGO, PVP/CHGO and PEG/CHGO.

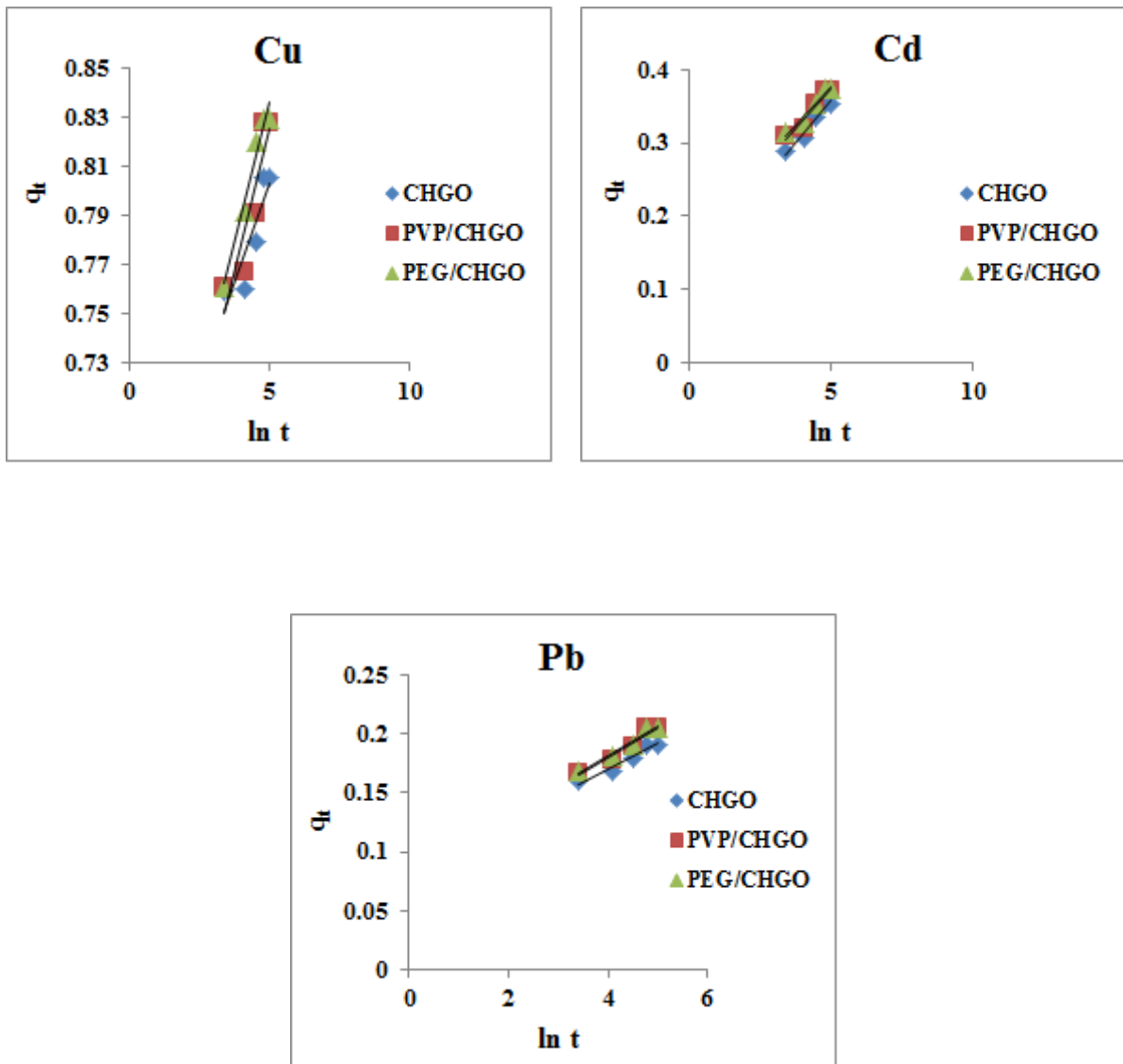


Fig.10. Elovich –kinetic model for the adsorption of removal, Cu, Cd and Pd metal ions with CHGO, PVP/CHGO and PEG/CHGO nanocomposite

Table 1 Kinetic Parameters of Cu metal ions

Adsorbent	$q_{e(\text{exp})}$	Pseudo-first order kinetic			Pseudo-second order kinetic			Elovich kinetic model		
		$q_{e(\text{cal})}$	K_1	R^2	$q_{e(\text{cal})}$	K_2	R^2	β	α	R^2
CHGO	0.8055	0.0679	0.0097	0.7697	0.8255	0.3053	0.9993	30.5810	10.1198	0.8122
PVP/CHGO	0.8278	0.0971	0.0099	0.8763	0.8565	0.2112	0.9988	21.4592	15.1673	0.8482
PEG/CHGO	0.8293	0.2112	0.0332	0.9506	0.8528	0.3004	0.9999	21.7391	24.0599	0.9665

Table 2 Kinetic parameters of Cd metal ions

Adsorbent	$q_{e(\text{exp})}$	Pseudo-first order kinetic			Pseudo-second order kinetic			Elovich kinetic model		
		$q_{e(\text{cal})}$	K_1	R^2	$q_{e(\text{cal})}$	K_2	R^2	β	α	R^2
CHGO	0.8055	0.0679	0.0097	0.7697	0.8255	0.3053	0.9993	30.5810	10.1198	0.8122
PVP/CHGO	0.8278	0.0971	0.0099	0.8763	0.8565	0.2112	0.9988	21.4592	15.1673	0.8482
PEG/CHGO	0.8293	0.2112	0.0332	0.9506	0.8528	0.3004	0.9999	21.7391	24.0599	0.9665

Table 3 kinetic parameters of Lead metal ions

Adsorbent	$q_{e(\text{exp})}$	Pseudo-first order kinetic			Pseudo-second order kinetic			Elovich kinetic model		
		$q_{e(\text{cal})}$	K_1	R^2	$q_{e(\text{cal})}$	K_2	R^2	β	α	R^2
CHGO	0.1910	0.0524	0.0154	0.9383	0.2046	0.4530	0.9975	47.6190	1.0228	0.9314
PVP/CHGO	0.2046	0.0588	0.0138	0.9930	0.2213	0.3619	0.9966	39.3701	0.5370	0.9429
PEG/CHGO	0.2049	0.0609	0.0161	0.9891	0.9978	0.3958	0.9978	40.8163	0.7252	0.9595

Based on the analysis of the R^2 of the linear form for various kinetics models as shown in table 1 to 3, the pseudo second order model was more appropriate than other models to describe the adsorption kinetics behaviour for all metal ions [Cu(II), Cd(II) and Pb(II)] onto the twenty four different adsorbents. The theoretical simulated curve as thin solid lines fitted the experimental data quite well, indicating a pseudo-second-order kinetic of metal ions of different adsorbent, and the chemisorptions were the rate controlling mechanism[45-47](Mohanty et al., 2005; Srivastava et al., 2006; Radhika et al., 2006).

Besides, the correlation coefficient of pseudo – first order model and elovich model were also almost higher than 0.9 which are shown in table 1 to 3, indicating that the adsorption mechanism based on these models may be partially involved in the adsorption process together with that of pseudo – second order kinetics.

6. CONCLUSION

Graphene Oxide (GO) was prepared from naturally available agricultural material coconut husk. The PVP/CHGO and PEG/CHGO were prepared by solution mixing of PVP with CHGO and PEG with CHGO. Grapheme Oxide and its polymeric composites were act as excellent adsorbent materials for the removal of heavy metals from simulated waste water. The adsorption study of metal ion by CHGO, PVP/CHGO and PEG/CHGO nanocomposite was shown to depend significantly on the pH, adsorbent dosage, contact time and initial metal ion concentration. The study further demonstrated that the adsorption process was of pseudo – first order kinetic model, pseudo – second order kinetic model and elovich kinetic model. The pseudo – second order kinetic model is better fitting in removal of metal ions. This methodology can be applied to the removal of toxic metals from wastewater efficiently. Moreover, efficient reuse of the regenerated bio-adsorbent was found to be possible. The method was simple, cost effective and environmental friendly.

ACKNOWLEDGEMENT

The authors sincerely thank the Principal, Presidency College, Chennai, Tamilnadu, for providing access to DST-FIST (SR/FIST/COLLEGE-098/2012) facility.

REFERENCES

1. Mao, H.Y., Laurent, S., Chen, W., Akhavan, O., Imani, M., Ashkarran, A.A., Mahmoudi, M., 2013. Graphene: Promises, facts, opportunities, and challenges in nanomedicine. *Chem. Rev.*113, 3407–3424. <https://doi.org/10.1021/cr300335p>.
2. Eigler, S., Hu, Y., Ishii, Y., Hirsch, A., 2013. Controlled functionalization of graphene oxide with sodium azide. *Nanoscale.* 5, 12136–12139. <https://doi.org/10.1039/C3NR04332K>.
3. Georgakilas, V., Otyepka, M., Bourlinos, A.B., Chandra, V., Kim, N., Kemp, K.C., Hobza, P., Zboril, R., Kim, K.S., 2012. Functionalization of graphene: Covalent and non-covalent approaches, derivatives and applications. *Chem. Rev.*112, 6156–6214. <https://doi.org/10.1021/cr3000412>.
4. Novoselov, K.S., Fal'ko, V.I., Colombo, L., Gellert, P.R., Schwab, M.G., Kim, K., 2012. A roadmap for grapheme. *Nature.* 490, 192–200. <https://doi.org/10.1038/nature11458>.
5. Chung, C., Kim, Y.K., Shin, D., Ryoo, S.R., Hong, B.H., Min, D.H., 2013. Biomedical applications of graphene and graphene oxide. *Acc. Chem. Res.*46, 2211–2224. <https://doi.org/10.1021/ar300159f>.
6. Brodie, B.C., On the atomic weight of graphite. *Philos. Trans. R. Soc. Lond.* 1859, 149, 249–259.
7. Staudenmaier, L., 1898. Verfahren zur Darstellung der Graphitsäure. *Ber. Dtsch. Chem. Ges.* 31, 1481–1487.
8. Hummers, W.S., Offeman, R.E., 1958. Preparation of graphitic oxide. *J. Am. Chem. Soc.* 80, 1339. <https://doi.org/10.1021/ja01539a017>.
9. Guo, S., Dong, S., 2011. Graphene nanosheet: Synthesis, molecular engineering, thin film, hybrids, and energy and analytical applications. *Chem. Soc. Rev.*40, 2644–2672. <https://doi.org/10.1039/C0CS00079E>.
10. Seo, D.H., Rider, A.E., Kumar, S., Randeniya, L.K., Ostrikov, K., 2013a. Vertical graphene gas- and bio-sensors via catalyst-free, reactive plasma reforming of natural honey. *Carbon.*60, 221–228. <https://doi.org/10.1016/j.carbon.2013.04.015>
11. Seo, D.H.; Han, Z.J.; Kumar, S.; Ostrikov, K. 2013b. Structure-controlled, vertical grapheme-based, binder-free electrodes from plasma-reformed butter enhance super capacitor performance. *Adv. Energy Mater.* 2013b, 10, 1316–1323. <https://doi.org/10.1002/aenm.201300431>.

12. Thirunavukkarasu Somanathan., Karthika Prasad., Kostya (Ken) Ostrikov., Arumugam Saravanan., Vemula Mohana Krishna., 2015. Graphene Oxide Synthesis from Agro Waste. *Nanomaterials*. 5, 826- 834. <https://doi.org/10.3390/nano520826>.
13. Aswini, K., Jaisankar, V., 2017. Preparation and Characterisation of Activated Carbon from Rice Husk and its Polyvinylpyrrolidone (PVP) Composite for Heavy Metal Removal from Simulated Wastewater. *JoWPPR*. 4(3), 10-15.
14. Aswini, K., Jaisankar, V., 2018. A Study on the Environmental Applications of Activated Carbon and Its Polymer Composite from Agro Waste Materials. *IJRAT*. 6(12), 3557- 3566.
15. Aswini, K., Jaisankar, V., 2019. Adsorption treatment of Heavy Metal removal from Simulated waste water using Rice Husk Activated Carbon (RHAC) and its polyvinylpyrrolidone (PVP) composite as an Adsorbent. *J. Wat. Env. Sci. Vol. 3 (1)*, 460-470.
16. Lokendra Singh Thakur., Pradeep Semil., 2013. Adsorption of Heavy Metal (Cd²⁺, Cr⁶⁺ and Pb²⁺) from Synthetic Waste Water by Coconut husk Adsorbent. *Int. J. Chem.* 1(4), 64-72.
17. Jothi Ramalingam, S., HidayathullaKhan, T., Pugazhenth, M., Thirumurugan, V., 2013. Removal of Pb (II) and Cd (II) ions from Industrial waste water using Calotropis Procera roots. *IJESI*. 2(4), 01-06.
18. Jayantakumarmaji, shukla,V.J., 2014. Simultaneous uv –visiblespectrophotometric quantitative determination of heavy metal ions using calibration method of proposed anti-hyperglycaemic formulation using cyaniding as a chromogenic reagent. *IJUPBS*. 3(5), 229-336.
19. Stankovich, S., Dikin, D.A., Piner, R.D., Kohlhaas, K.A., Kleinhammes, A., Jia, Y., Wu, Y., Nguyen, S.T., Ruoff, R.S., 2007. Synthesis of graphene-based nanosheets via chemical reduction of exfoliated graphite oxide. *Carbon*, 45, 1558-1565. <https://doi.org/10.1016/j.carbon.2007.02.034>.
20. Tuinstra, F., Koenig, J.L., 1970. Raman Spectrum of Graphite. *J. Chem. Phys.* 53, 1126-1130. <https://doi.org/10.1063/1.1674108>.
21. Eda, G., Fanchini, G., Chhowalla, M., *Nat Nanotechnol.*, 2008. Large-area ultrathin films of reduced graphene oxide as a transparent and flexible electronic material. 3(5), 270-274. <https://doi.org/10.1038/nnano.2008.83>.

22. Calizo, I., Balandin, A.A., Bao, W., Miao, F., Lau, C.N., 2007. Temperature Dependence of the Raman Spectra of Graphene and Graphene Multilayers. *Nano Lett.*, 7(9) 2645-2649. <https://doi.org/10.1021/nl071033g>.
23. Kudin, K.N., Ozbas, B., Schniepp, H.C. Prudhomme, R.K, Aksay, I.A., Car, R., 2008. Raman spectra of graphite oxide and functionalized graphene sheets. *Nano Lett.* 8, 36. <https://doi.org/10.1021/nl071822y>.
24. Gebremedhin Gebrehawaria., 2016. Removal of Chromium (VI) Ions from Aqueous Solution Using Leaves of Cordia Africana and Sawdust of Acacia Albida. *Int. j. modern chem. appl. sci.* 3(2): 369-377.
25. Ahmad Monshi., Mohammad Reza Foroughi., Mohammad Reza Monshi., 2015. Modified Scherrer Equation to Estimate More Accurately Nano-Crystallite Size Using XRD. *WJNSE.* 2, 154-160. <https://doi.org/10.4236/wjnse.2012.23020>.
26. Muralidharan, M.N., Ansari, S., 2013. Thermally reduced graphene oxide/thermoplastic polyurethane nanocomposites as photomechanical actuators. *Adv. Mater. Lett.*, 4(12), 927-932. <https://doi.org/10.5185/amlett.2013.5474>.
27. Kellici, S., Acord, J., Ball, J., Reehal, H.S., Morgan, D., Saha, B., 2014. A single rapid route for the synthesis of reduced graphene oxide with antibacterial activities. *RSC Adv.* 4, 14858-14861. <https://doi.org/10.1039/C3RA47573E>.
28. Chun, O.W.; Chen, M.L.; Zhang, K.; Zhang, F.J. The effect of thermal and ultrasonic treatment on the formation of graphene-oxide nanosheets. *J. Korean Phys. Soc.* 2010, 56, 1097–1102.
29. Bo, Z., Shuai, X., Mao, S., Yang, H., Qian, J., Chen, J., Yan, J., Cen, K., 2014. Green preparation of reduced graphene oxide for sensing and energy storage applications. *Sci. Rep.* 4, 1–5. <https://doi.org/10.1038/srep04684>.
30. Kaniyoor, A.; Ramaprabhu, S., 2012. A Raman spectroscopic investigation of graphiteoxide derived graphene. *AIP Adv.* 2, 032183- 13. <https://doi.org/10.1063/1.4756995>.
31. Eigler, S.; Dotzer, C.; Hirsch, A., 2012. Visualization of defect densities in reduced graphene oxide. *Carbon.* 50, 3666–3673. <https://doi.org/10.1016/j.carbon.2012.03.039>.
32. Ansari, R., 2006. *Acta ChimSlov.*, 2006. Application of Polyaniline and its Composites for Adsorption/Recovery of Chromium (VI) from Aqueous Solutions. 53, 88–94.
33. Raffieabaseri, J., Palanisamy, P.N., Sivakumar, P., *E-J CHEM.*, 2012; 9: 1122.

34. Garg, V.K., Gupta, R., Yadav, A.B., R.D. Kumar, R.D., 2003. Dye removal from aqueous solution by adsorption on treated sawdust. *Bioresour. Tech.*, 89(2): 121 – 124. [https://doi.org/10.1016/S0960-8524\(03\)00058-0](https://doi.org/10.1016/S0960-8524(03)00058-0).
35. Najua, D.T., Luqman, C.A., Zawani, Z., Suraya, A.R., 2008. Adsorption of copper from aqueous solution by *ElaisGuineensis* kernel activated carbon, *J. Eng. Sci. Tech.* 2(1), 180-189.
36. Gayathri, R., Thirumarimurugan, M., Kannadasan, T., 2013. A study on adsorption of chromium (VI) ions from aqueous solution by *Ficus religiosa* leaves as adsorbent *Pelagia research library.* 4(3), 79-87.
37. Shams Khorramabadi, G., DarvishiCheshmehSoltani, R., Jorfi, S., 2010. Cd (II) adsorption using waste sludge from a municipal wastewater treatment system. *Journal of Water and Wastewater*, 21 (1), 57-62. (In Persian)
38. Lagergren, S., 1898. Zurtheorie der sogenannten adsorption gel^sterstoffe, *Kungliga Svenska Vetenskapsakademiens. Handlingar*, 24 (4), 1-39.
39. Qiu, H., Lv, L., Pan, B.C., Zhang, Q., Zhang, W., Zhang, Q., Zhejiang, J., *Univ. Sci. A*, 2009;Critical review in adsorption kinetic models.10, 716-724. <http://dx.doi.org/10.1631/jzus.A0820524>.
40. Fan, X., Parker, D.J., Smith, M.D., 2003. Adsorption kinetics of fluoride on low cost materials. *WaterResearch.*37,4929-4937. <http://dx.doi.org/10.1016/j.watres.2003.08.014>.
41. Ho, Y., 2006. Review of second-order models for adsorption systems. *J. Hazard. Mater.*, 136, 681-689. <http://dx.doi.org/10.1016/j.jhazmat.2005.12.043>.
42. Ho, Y.S., McKay, G., 1998. Sorption of dye from aqueous solution by peat. *Chem. Eng. J.*, 70, 115-124. [http://dx.doi.org/10.1016/S0923-0467\(98\)00076-1](http://dx.doi.org/10.1016/S0923-0467(98)00076-1).
43. Juang, R.S., Wu, F.C., Tseng, R.L., 2000. Mechanism of Adsorption of Dyes and Phenols from Water Using Activated Carbons Prepared from Plum Kernels. *J. Colloid Interf. Sci.*, 2000; 227(2), 437-444. <http://dx.doi.org/10.1006/jcis.2000.6912>.
44. Hameed, B.H., 2009. Evaluation of papaya seeds as a novel non-conventional low-cost adsorbent for removal of methylene blue. *J. Hazard. Mater.* 162, 939-944. <http://dx.doi.org/10.1016/j.jhazmat.2008.05.120>.
45. Mohanty, K., Das, D., Biswas, M.N., 2005. Adsorption of phenol from aqueous solutions using activated carbons prepared from *Tectona grandis* sawdust by ZnCl₂ activation. *Chem.Eng.J.*, 2005; 115: 121-131. <http://dx.doi.org/10.1016/j.cej.2005.09.016>.

46. Srivastava, V.C., Swamy, M.M., Mall, I.D., Prasad, B., and Mishra, I.M., 2006. Adsorptive removal of phenol by bagasse fly ash and activated carbon: Equilibrium, kinetics and thermodynamics. *Colloids Surf. A.* 272, 89-104.
47. Radhika, M., Palanivelu, K., 2006. Adsorptive removal of chlorophenols from aqueous solution by low cost adsorbent-Kinetics and isotherm analysis. *J. Hazard. Mater.*, 138, 116-124. <http://dx.doi.org/10.1016/j.jhazmat.2006.05.045>.

Figures

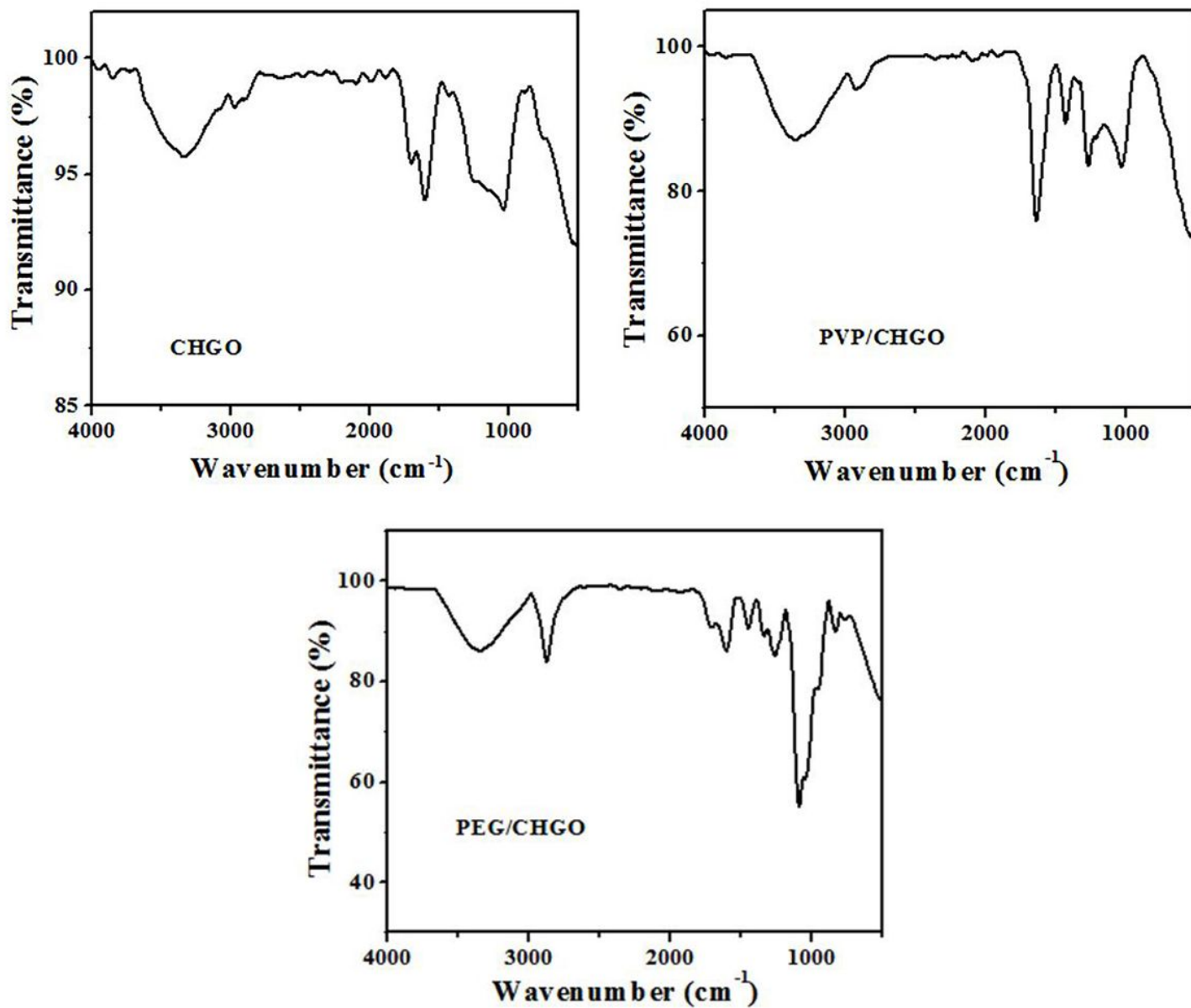


Figure 1

FT-IR spectra recorded for CHGO, PVP/CHGO and PEG/CHGO

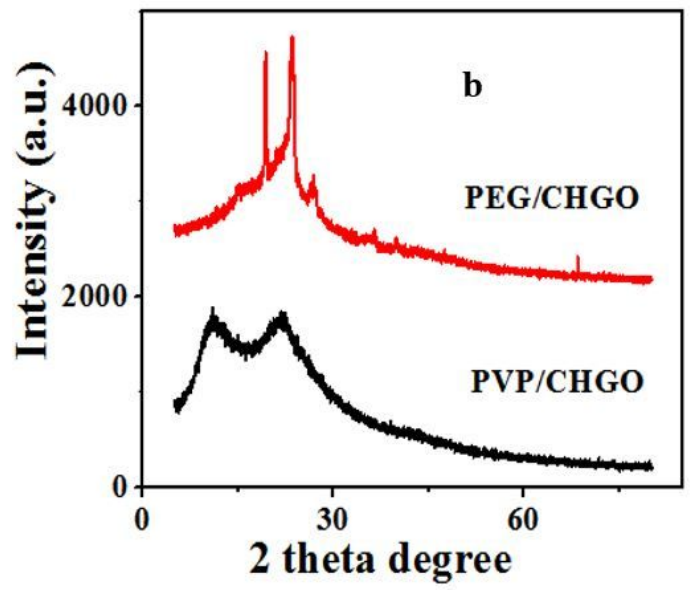
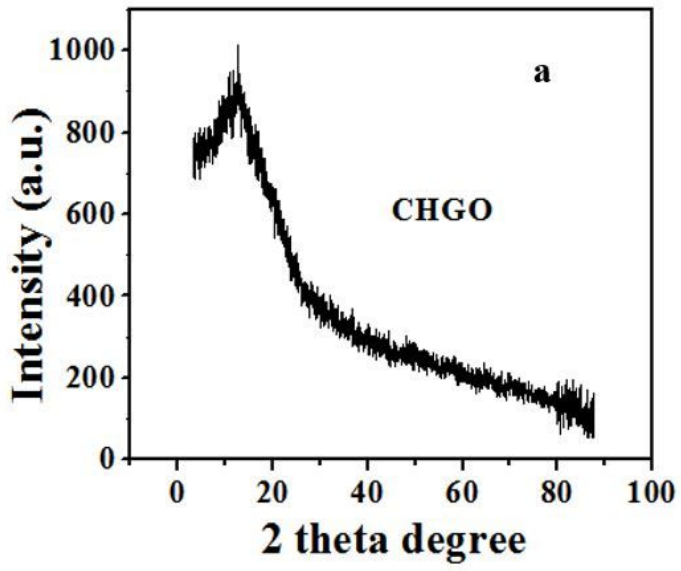


Figure 2

X-ray diffraction pattern of Coconut husk (a), CHGO, (b) PVP/CHGO and (c), PEG/CHGO

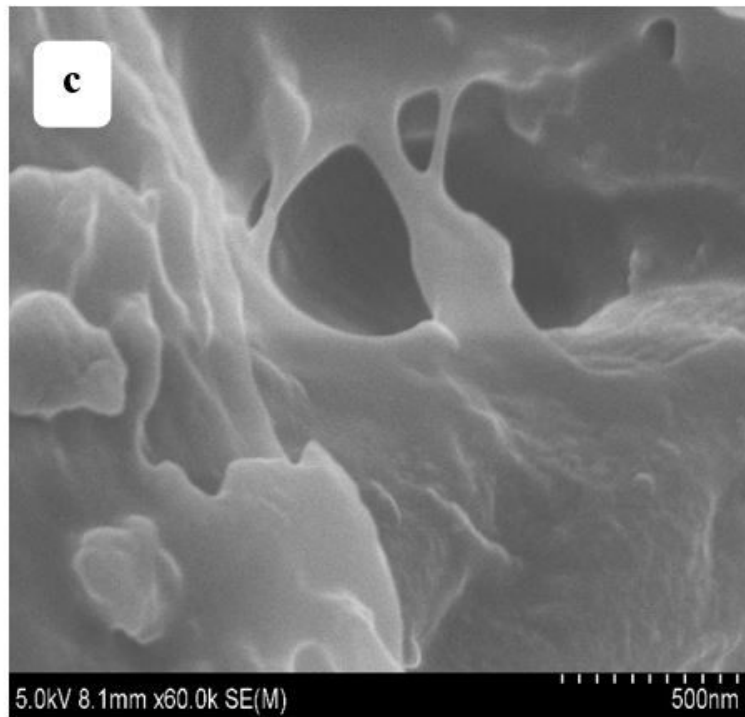
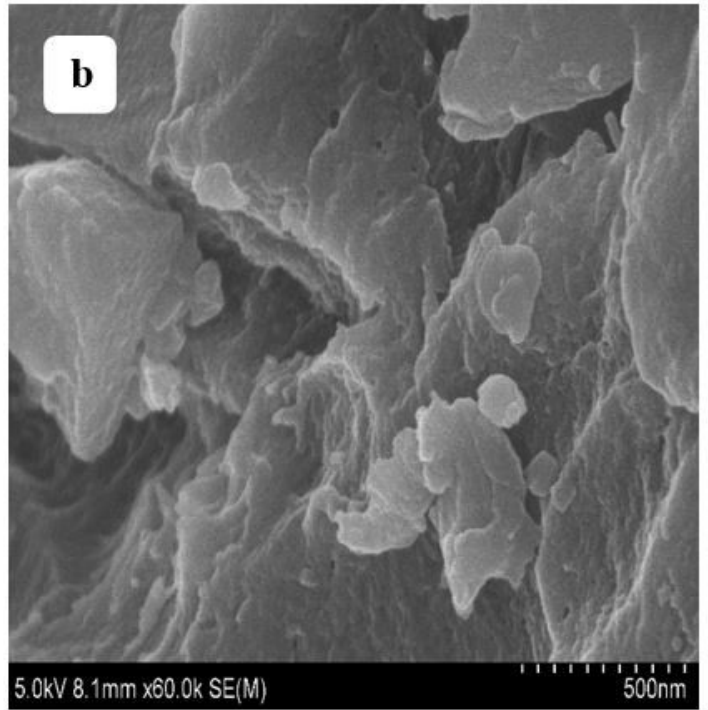
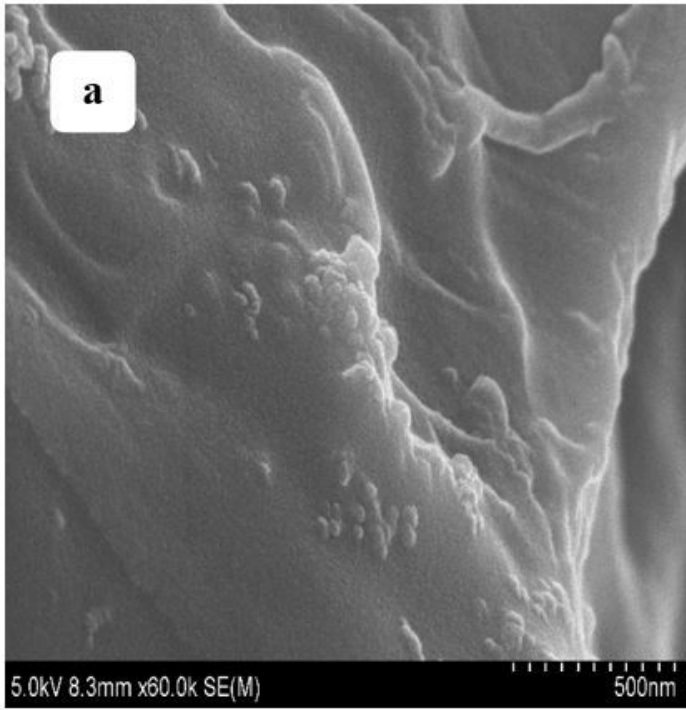


Figure 3

HRSEM images of (a) CHGO, (b) PVP/CHGO and (c) PEG/CHGO

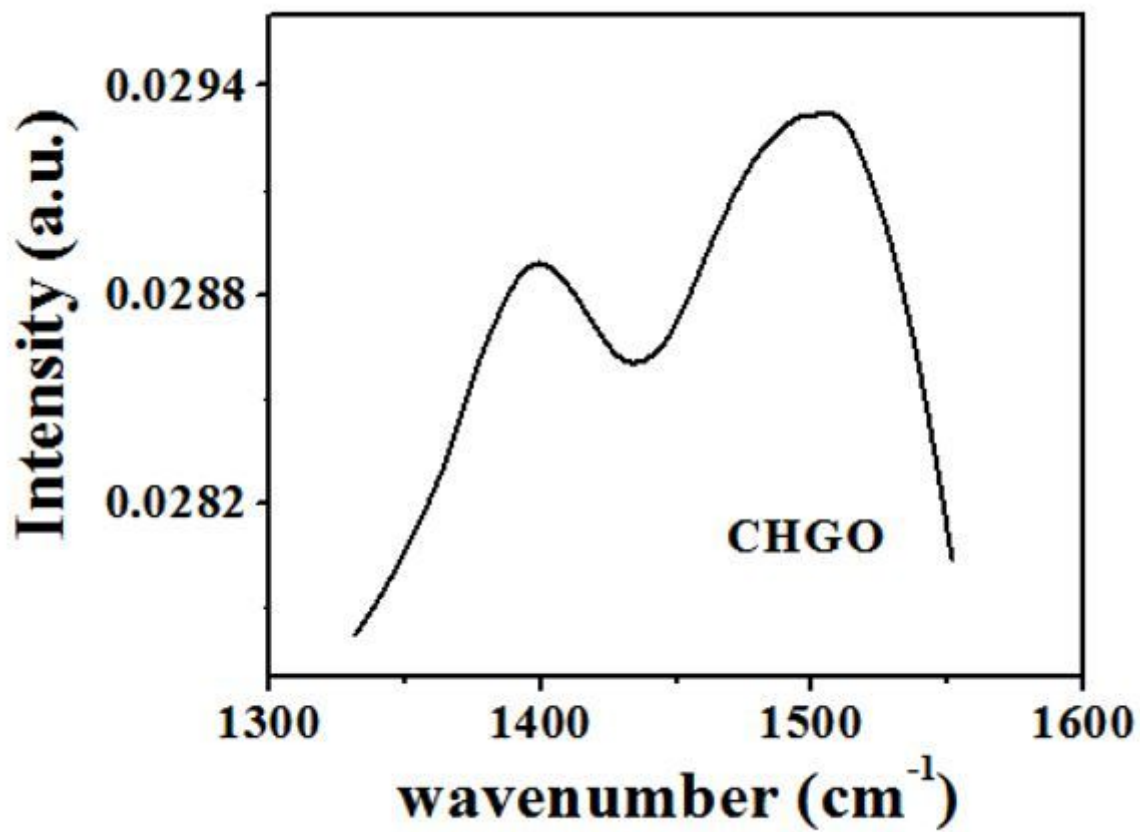


Figure 4

Raman spectrum of GO form Coconut husk (CHGO)

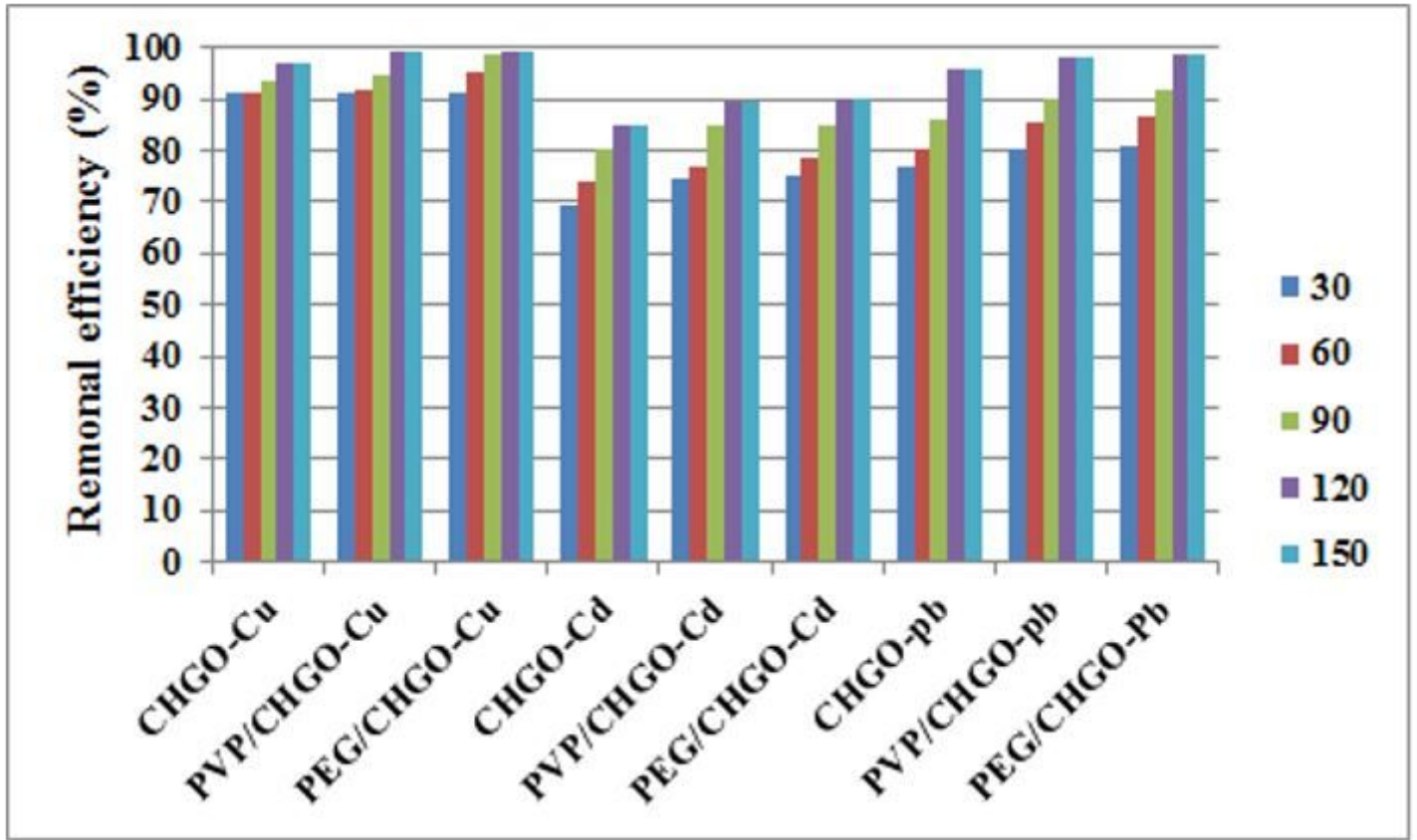


Figure 5

Effect of Contact time on adsorption of Lead, Copper and Cadmium metal ions pH=6 (dose= 0.6)

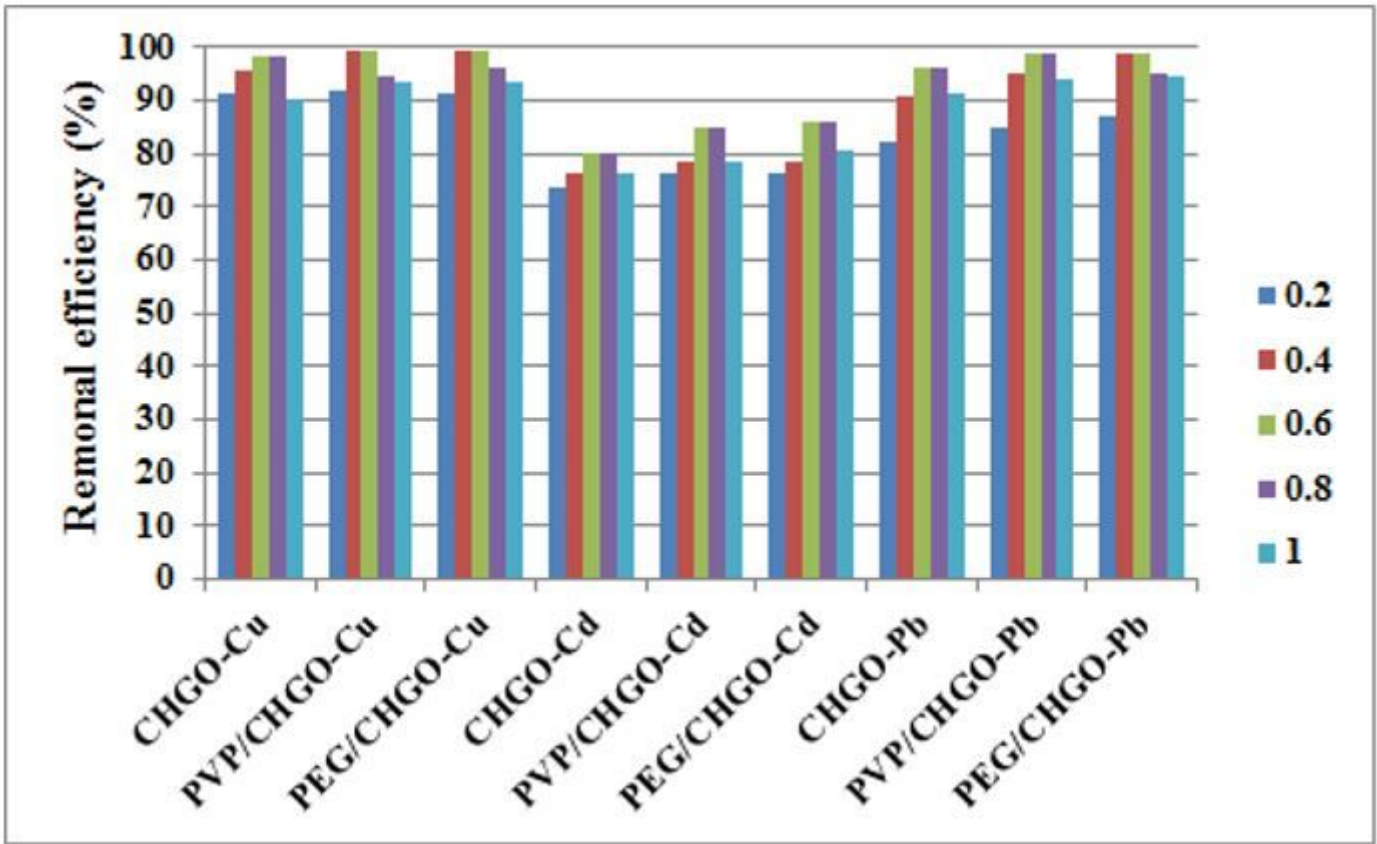


Figure 6

Effect of Adsorbent dosage on adsorption of Lead, Copper and Cadmium metal ions pH=6 (Contact time= 120)

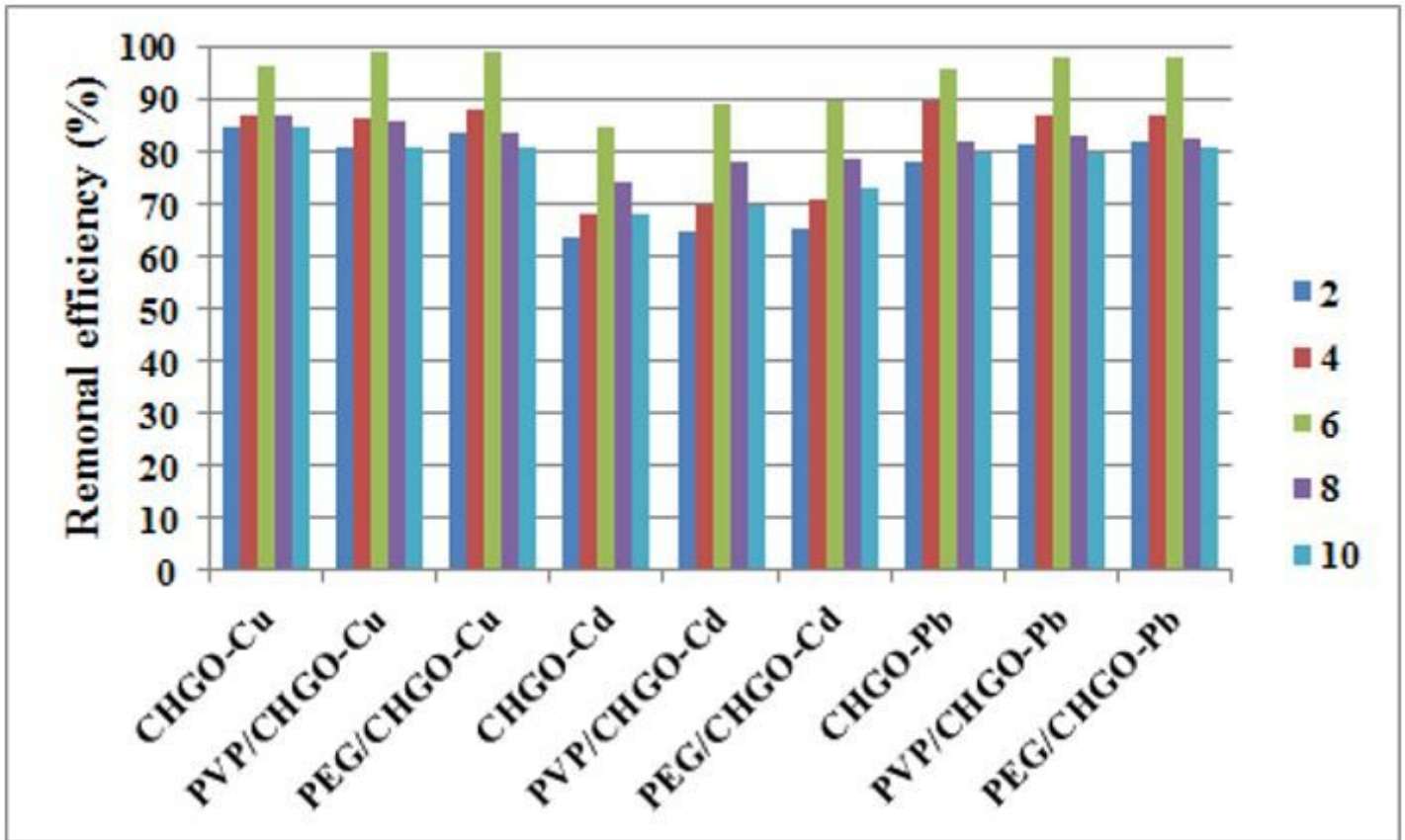


Figure 7

Effect of pH on adsorption of Lead, Copper and Cadmium metal ions pH=6 (dose= 0.6)

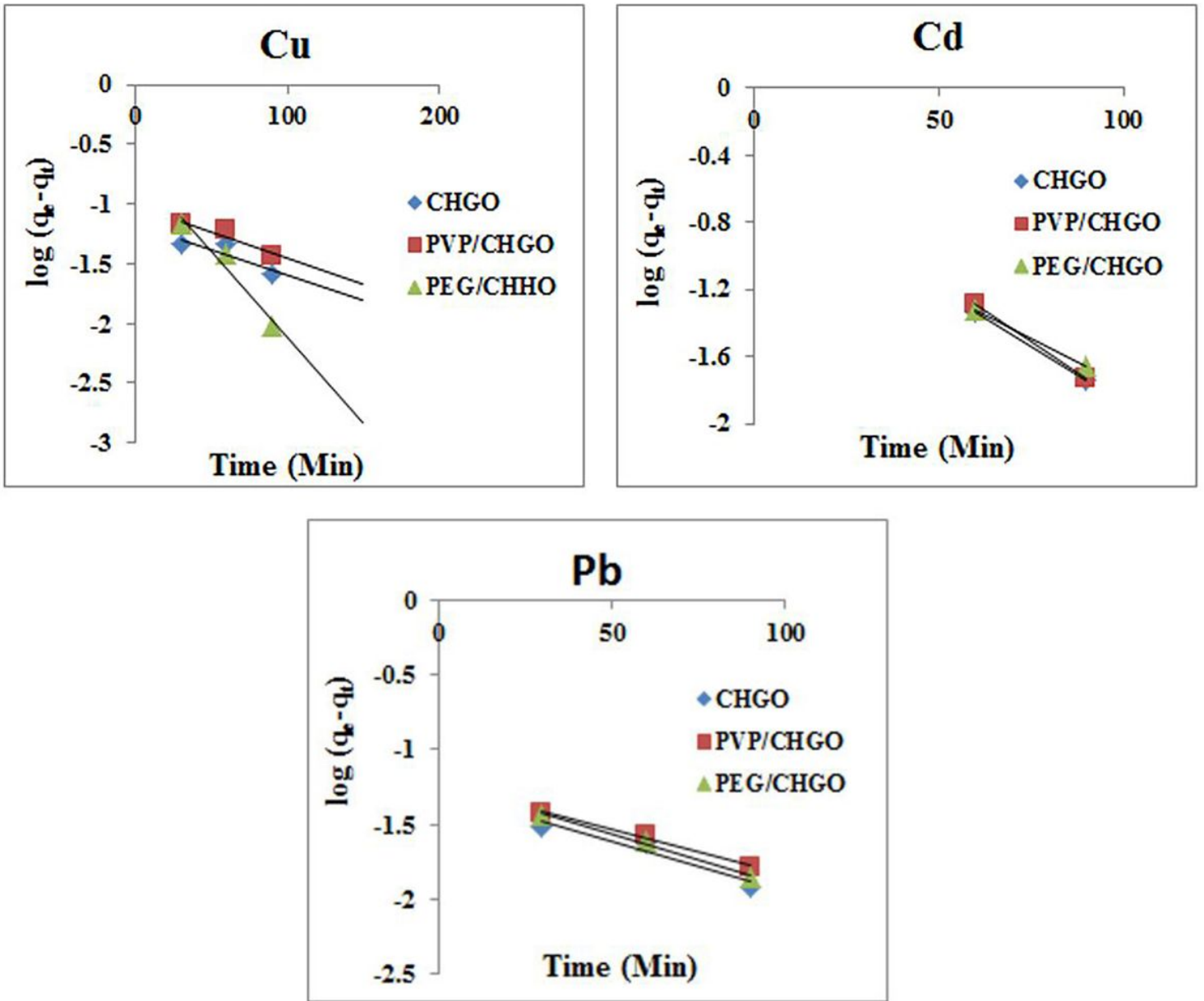


Figure 8

Lagergren first-order –kinetic model for the adsorption of removal Cu, Cd and Pb metal ions with CHGO, PVP/CHGO and PEG/CHGO nanocomposite

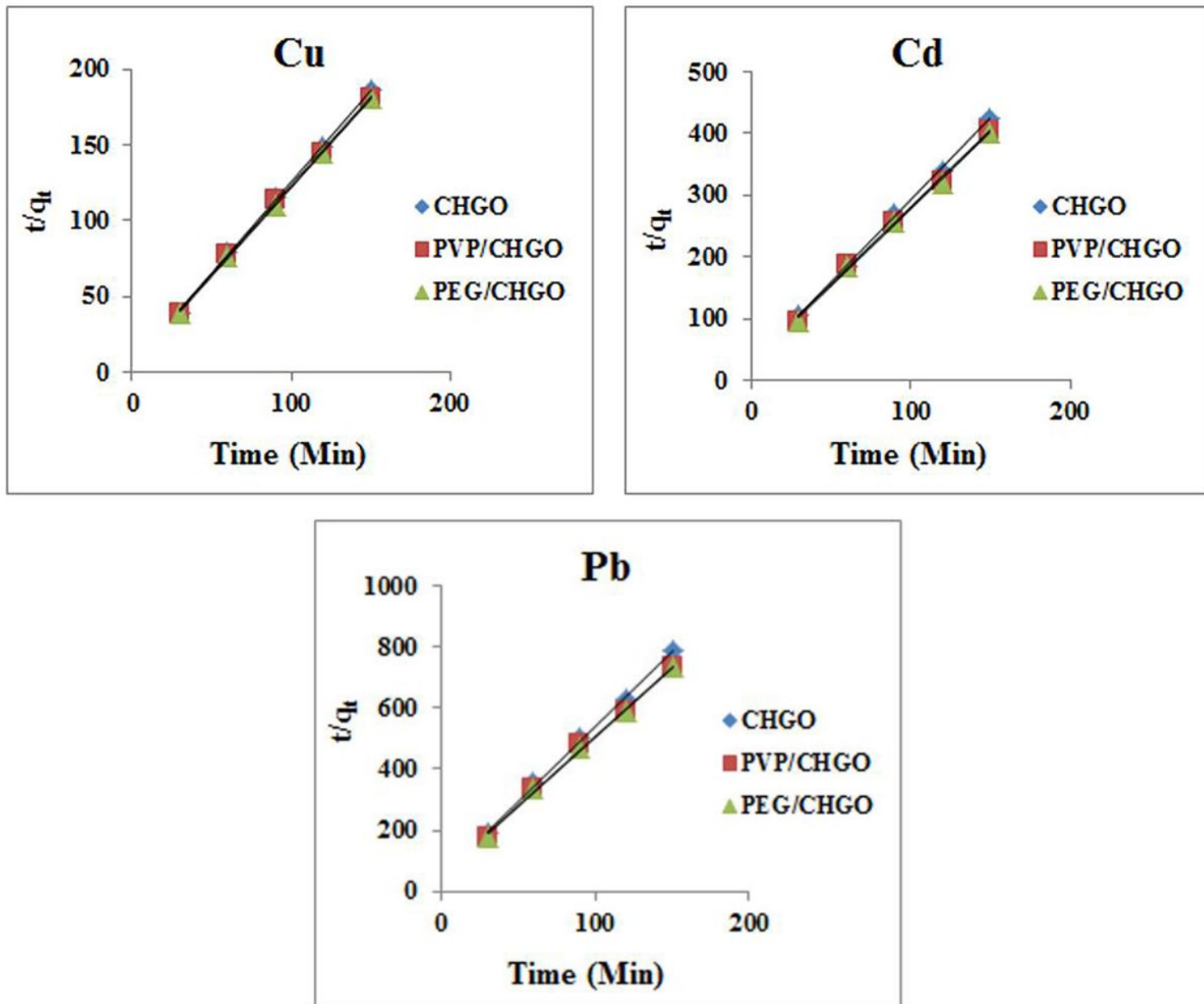


Figure 9

Pseudo second-order –kinetic model for the adsorption of removal Cu, Cd and Pb metal ions with CHGO, PVP/CHGO and PEG/CHGO nanocomposite

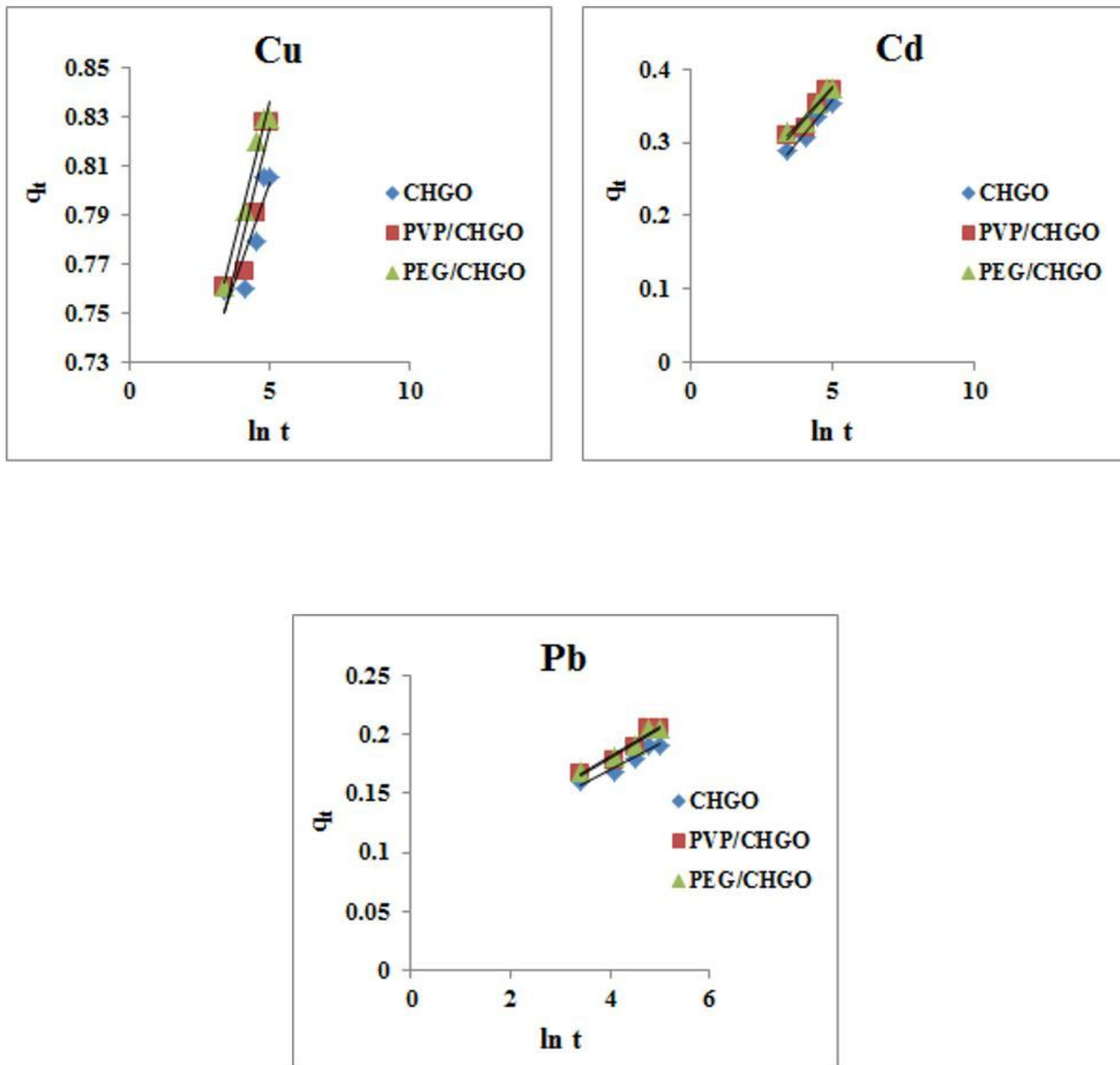


Figure 10

Elovich –kinetic model for the adsorption of removal, Cu, Cd and Pd metal ions with CHGO, PVP/CHGO and PEG/CHGO nanocomposite